Improved Gyrator-Capacitor Modeling of Magnetic Circuits with Inclusion of Magnetic Hysteresis

Hayerikhiyavi, Mohammadali and Dimitrovski, Aleksandar

University of Central Florida, University of Central Florida

2021

Improved Gyrator-Capacitor Modeling of Magnetic Circuits with Inclusion of Magnetic Hysteresis

Mohammadali Hayerikhiyavi, Aleksandar Dimitrovski
Department of Electrical and Computer Engineering
University of Central Florida
Orlando, USA
Mohammad.ali.hayeri@knights.ucf.edu, ADimitrovski@ ucf.edu

***Abstract*—Gyrator-Capacitor (G-C) models of electromagnetic devices provide a robust and convenient approach for simulation of a combined power device that consists of magnetic and electric/electronic circuits. The G-C model seamlessly links magnetic and electric/electronic sides of the device in a power invariant fashion which is very useful for integrated system analysis. This paper proposes an improved G-C model that includes hysteresis besides the core saturation for a ferromagnetic circuit. The approach has been applied to model a Continuously Variable Series Reactor (CVSR) with electromagnetic coupling between two circuits, a control dc and a controlled ac circuit. Taking into account the ferromagnetic core nonlinearities, the CVSR behaviour is investigated in terms of induced voltages across the windings and corresponding magnetic flux densities.**

***Index Terms*-- Continuously Variable Series Reactor (CVSR), Gyrator-Capacitor (G-C) model, hysteresis, magnetic amplifier.**

I. INTRODUCTION

Accurate modeling is vital to better understand the behavior of a power system and its components and helps their further development. This is particularly true in the case of nonlinear magnetic components that interact with the electrical domain [1, 2]. The typical approach in modeling of magnetic circuits is to use the electric circuit analogy of Ohm's Law. This approach results with equivalent circuits that use resistors to represent magnetic reluctances and voltage sources that represent magneto-motive forces (MMFs). These models do not interface directly with the models on the electric side for integrated simulations and study of the overall system. Moreover, there is a contradiction in modeling magnetic cores that store energy with dissipative components like resistors which destroys the energy and power equivalence.

In the Gyrator-Capacitor (G-C) model, the analogy between the MMF and the voltage is still kept, but the electric current is analog to flux rate (i.e., flux is analog to electric charge) and magnetic permeance is analog to capacitance. This model forms a direct link between the electrical and magnetic circuits, which makes it robust and convenient for integrated study of systems with power magnetic devices. For precise and accurate simulations, the magnetic component nonlinearities should also be considered in the model [3].

In a basic representation of the magnetic core, the core saturation is usually modeled without the hysteresis, i.e. the B-H curve loop, indicating a zero-loss system [4]. In order to provide a more comprehensive model, some work has been done on modeling core losses due to the hysteresis effect. One of those models is the Jiles-Atherton model (JA model [5]). Due to its complexity, this model may have convergence problems which makes it not so suitable for intensive dynamic studies. Moreover, in some cases, it may not provide accurate results. Other methods (Rayleigh, Frölich, Preisach, and Potter model) have been investigated for magnetic hysteresis modeling in [6], with comparison based on the accuracy and ease of implementation. Rayleigh provides an accurate enough model for the cores with high coercivity. Potter model uses simpler mathematical expression but, in some cases, has a significant error. The results obtained using Frölich and Preisach models are close to those from experiments, but they are also not very suitable for dynamic analysis.

In this paper, the hysteresis in the G-C model is modeled by adding a resistor in series with the core capacitor. The value of this resistor depends on the core material, its volume, and its specific losses. The model is quite suitable for both static and dynamic (transient) simulations. The improved G-C model of a Continuously Variable Series Reactor (CVSR) with nonlinear magnetic core including hysteresis and saturation, has been implemented in MATLAB/Simulink® and used as case study.

The basic concept of the CVSR is briefly reviewed in Section II. The gyrator-capacitor (G-C) approach in modeling magnetic circuits with nonlinearities, including core saturation and hysteresis, is explained in Section III. Section IV presents simulation results and analysis of the CVSR for different dc and ac voltage sources, with comparison of the hysteresis effect on its behavior, and conclusions are summarized in Section V.

II. CONTINUOUSLY VARIABLE SERIES REACTOR

A CVSR includes an ac winding wound on the middle leg of a three-legged magnetic circuit, connected in series with an

ac circuit that part of the power grid. Typically, an air gap in the middle leg is necessary to achieve the desired reactance in normal conditions and not to saturate the core for very small ac currents [7]. The air gap allows larger range of change for the ac reactance of the device. Two dc windings are wound on the outer legs and connected in series with opposite polarities. A controlled dc current establishes a dc flux passing through the outer legs and yokes. The ac reactance of the reactor is controlled by the current in the dc circuit [8]. This reactance reaches a maximum value when the core is in the linear region of the B-H curve (at zero or very small dc) and a minimum value when it is fully saturated (at large dc). The variable ac reactance controlled by the dc bias can be used for applications like power flow control, oscillation damping, and fault current limitation. At any instance of time, the ac and dc fluxes will add in one of the outer legs and subtract in the other as shown in Figure 1. After reaching the saturation point, the reluctance of the first leg will decrease and increase in the second. The induced voltages on the right and left dc winding will be $\frac{d\Phi_{right}}{dt}$ and $\frac{d\Phi_{left}}{dt}$, respectively, and the induced across the entire dc windings is: $V_{bias} = V_{right} - V_{left}$.

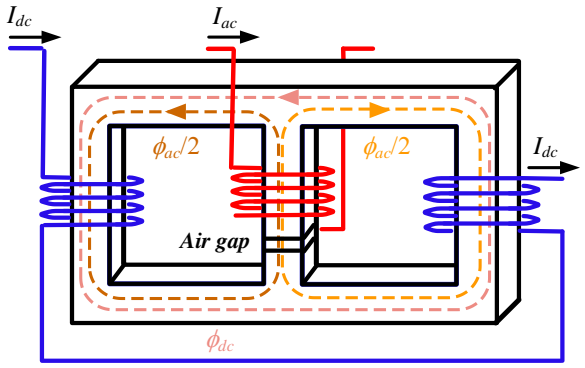

Fig. 1. Schematic of a CVSR

III. GYRATOR CAPACITOR MODEL

As mentioned above, the typical representation of magnetic circuits with analog electric circuits [9], where resistors represent flux paths and voltage sources represent MMFs, is inconsistent because it uses dissipative elements (resistors) to represent energy storage elements (magnetic cores). An energy-invariant approach is given by the G-C model shown in Figure 2 [10].

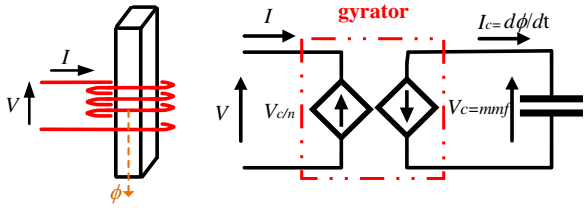

Fig. 2. Simple magnetic circuit and its equivalent gyrator-capacitor model

In the G-C approach, the analogy is between the MMF and the voltage, and the current and the rate-of-change of magnetic flux $\frac{d\Phi}{dt}$, as described by (1) and (2) [11]:

$$V_c \equiv mmf \tag{1}$$

$$I_c = \frac{d\Phi}{dt} \tag{2}$$

The gyrator operates as a dualizer allowing the voltage and current interchange based on the number of turns in the winding which defines its parameter (gyrator resistance).

A simple model of the CVSR using the G-C method as implemented in Simulink® is shown in Figure 3. Nonlinear permeances representing the nonlinear magnetic paths are modelled as nonlinear capacitors C_1, C_2, C_3, for the left, middle, and the right leg, respectively. The windings are represented with gyrators. A linear permeance (C_g) models the air gap in the middle leg. Any modelling of the fringing flux is also included in the air gap permeance [12]. The permeances can be calculated in a simple way from the material characteristics and geometric parameters as given by (3):

$$\rho = \frac{\mu_r \mu_0 l}{A} \tag{3}$$

where: μ_0 is the magnetic permeability of free air, μ_r is the relative permeability of the material, A is the cross-section area of the path, and l is the mean length of the path.

For a more accurate model of the CVSR, the hysteresis is modelled by adding a resistor in series with the corresponding core capacitor. These resistors (R_1, R_2, R_3) are illustrated in Figure 3. The values of these resistors depend on the core geometry, material, and its specific losses.

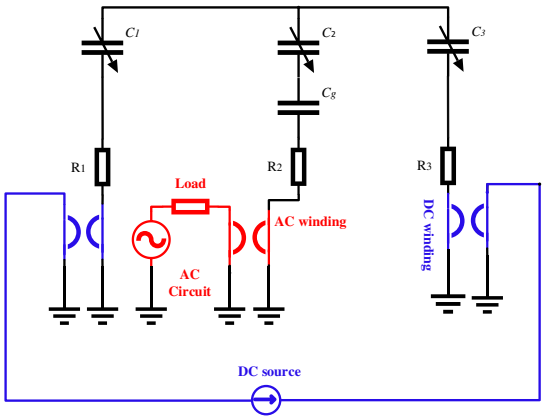

Fig. 3. Gyrator-Capacitor model in Simulink®

IV. SIMULATIONS AND RESULTS

A CVSR with parameters listed in Table I has been used as case study. The ferromagnetic core was assumed to be M36 with details given in [13]. All the modeling and simulation has been done in Simulink [14].

The model of the CVSR shown in Figure 3 is based on its electromagnetic circuit shown in Figure 1. The dc circuit is controlled by a dc source and the two gyrators on both sides represent each of the dc windings. The gyrator in the middle represents the ac winding. The ac circuit consists of a load and a voltage source. Both the basic and the improved G-C models of the CVSR have been studied under normal conditions for different dc bias currents. The CVSR behavior in terms of induced voltages across the windings and magnetic flux densities (B) throughout the core are presented.

Table I – CVSR PARAMETERS

Parameter	Description	Value
l_m	mean length of the middle leg	45.72 cm
l_{out}	mean length of the outer legs	86.36 cm
h_{ag}	height of the air gap	0.1780 cm
A	cross-section area of the core	0.0103 m^2
N_{dc}	number of turns in the dc winding	100
N_{ac}	number of turns in the ac winding	50
V	voltage source	2.4 kV
R	load resistance	100 Ω
L	load inductance	130 mH
B_{sat}	saturation point	1.34 T

A. *CVSR analysis without hysteresis*

Four different dc bias currents are applied in this scenario: 0 A, 200 mA, 2 A, and 10 A. These currents are characteristic ones that show different normal operating conditions of the CVSR.

The flux densities (magnetic inductions) and the terminal voltage (induced voltage across the ac winding) for 0 A dc bias are shown in Figures 4 and 5, respectively. The flux densities are purely sinusoidal and, therefore, the terminal voltage is also purely sinusoidal. The flux densities in the outer legs are equal to each other and the induced voltages in the two dc windings cancel each other due to the opposite polarities. Hence, the equivalent voltage across them is zero (Figure 6). This voltage is equivalent to the difference between the flux rates of the two outer legs:

$$E_{emf} = N_{dc}.\left(\frac{d\Phi_{right}}{dt} - \frac{d\Phi_{left}}{dt}\right) \quad (4)$$

E_{emf}: induced voltage

N_{dc}: Number of DC turns of dc winding

$\frac{d\Phi}{dt}$: Flux rate

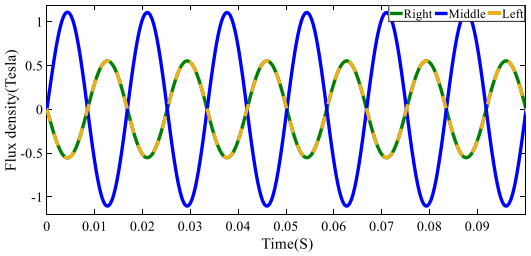

Fig. 4. Flux densities through CVSR (I_{dc} =0A)

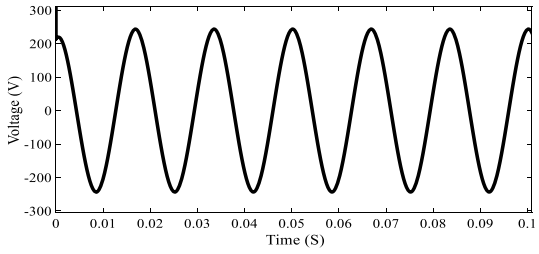

Fig. 5. Induced voltage across the ac winding (I_{dc} = 0 A)

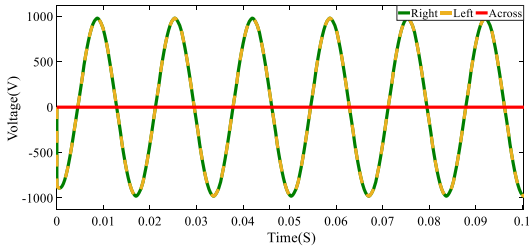

Fig. 6. Induced voltage across the dc winding (I_{dc} = 0 A)

The B-H characteristic for the middle leg of the CVSR at 0 dc bias is shown in Figure 7. As expected, it is a straight line since the core is unsaturated and hysteresis has not been modelled.

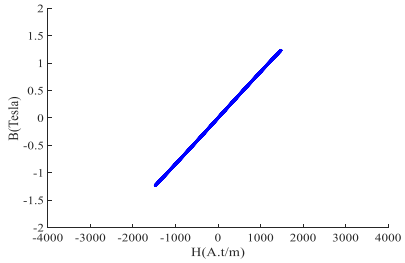

Fig. 7.B-H characteristic

The current through the ac winding shown in Figure 8 is directly obtained from the voltage source and the equivalent ac circuit impedance. The latter consists of the load impedance and the equivalent reactance of the CVSR in series. The expression for calculating the equivalent inductance of the CVSR is given by (5):

$$L = \frac{N_{ac}^2}{R_m} \quad (5)$$

R_m – equivalent reluctance of the device

N_{ac}: Number of AC turns of dc winding

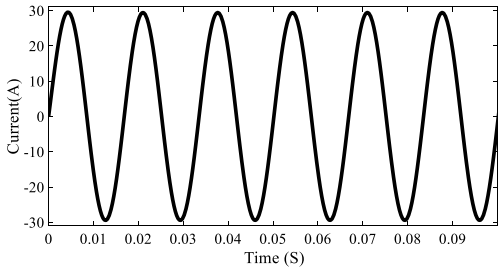

Fig. 8. Current in the ac winding (I_{dc} = 0 A)

Figure 9 shows the flux densities when the dc circuit has a dc bias of 200 mA. This results with an offset in the outer legs flux densities. They are no longer identical, but they are still in phase. So, the induced voltage across the dc windings will still be zero as shown in Figure10.

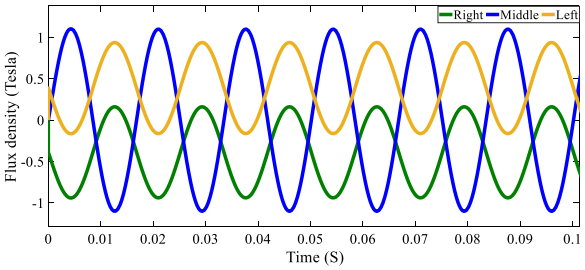

Fig9. Flux densities through CVSR (I_{dc} =200 mA)

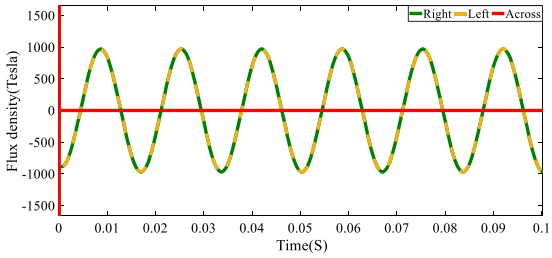

Fig. 10. Induced voltage across the ac winding (I_{dc} = 200 mA)

Since the CVSR still works in the non-saturation region, the equivalent inductance of the CVSR will not be changed in comparison to the previous case. The induced voltage across the ac winding and the ac current are the same as in the previous case (0A dc).

Figure 11 shows the flux densities for a dc bias of 2A. This is a critical current at which one of the outer legs is in saturation and the other is unsaturated. The induced voltage across the ac winding is distorted, as shown in Figure 12. The induced voltage across the dc windings is non-zero and has a frequency twice of the system, as shown in Figure 13.

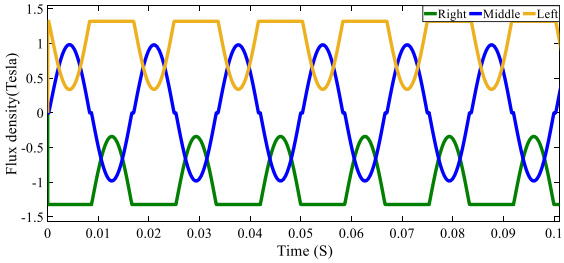

Fig11.Flux densities through CVSR legs (I_{dc} =2A)

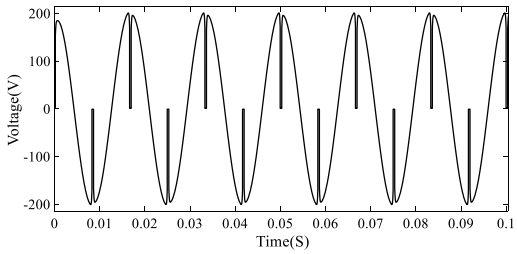

Fig12. Induced voltage across the ac winding (I_{dc} = 2 A)

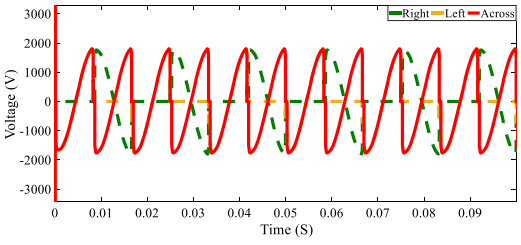

Fig13. Induced voltage across the dc windings (I_{dc} = 2 A)

Figure14 shows the case when the core goes completely into saturation due to the high dc bias current (10 A), and the magnetic induction through the middle leg is heavily decreased due to the high reluctance of the outer legs that complete the magnetic circuit. The induced voltage across ac winding is miniscule due to the minimal value of flux change through the middle leg.

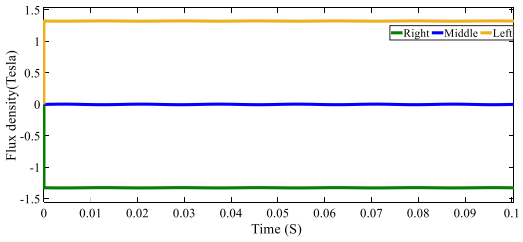

Fig14. Flux densities through CVSR legs (I_{dc} =10A)

Due to the same reason, the equivalent reactance in the ac circuit will be negligible and the current in the ac winding is equal to the full load current. This current is higher than in the previous cases because the equivalent inductance of the CVSR reaches its minimum value when fully saturated.

Also, since the outer legs are fully saturated, the induced voltages on the outer legs are equal and, the induced voltage across the dc windings will be zero.

B. CVSR analysis with hysteresis

The same four different dc bias currents are applied as in the previous scenario (0 A, 200 mA, 2 A, and 10 A), but this time in presence of hysteresis. Comparisons of the results show how hysteresis can affect the CVSR behavior.

The B-H characteristic for the middle leg of the CVSR at 0 dc bias is shown in Figure 15. If the solution of the magnetic equivalent circuit is given in terms of flux densities B, based on the expressions of the G-C model, the field intensity H is obtained directly from the voltage across the corresponding leg and its length.

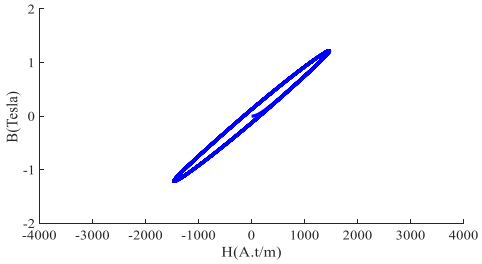

Fig15. B-H characteristic

The flux densities at 0 A dc bias are presented in Figure 16. Again, the ac flux is divided equally between the outer legs, and the flux densities through them are equal. Therefore, the induced voltages in the two dc windings cancel each other and the equivalent voltage across them is zero.

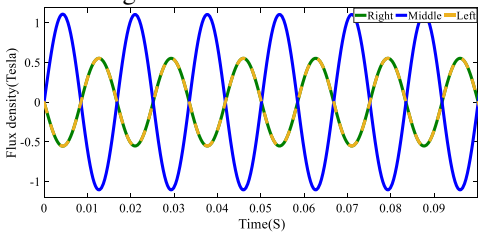

Fig16. Flux densities through CVSR (I_{dc} =0A)

In Figures 17 and 18, the flux densities and the induced voltage across dc windings are shown at a dc bias equal to 200 mA. Again, there is an offset in the outer legs inductions and they are no longer identical. However, in comparison to the previous case at the same dc bias (without hysteresis), they are

also no longer in phase because of the hysteresis. Therefore, the induced voltage across dc windings will not be zero anymore.

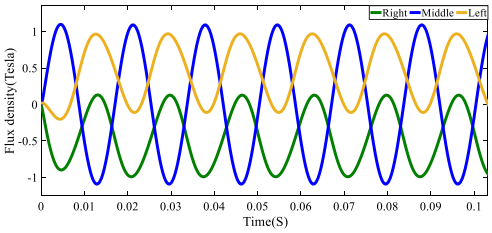

Fig17. Flux densities through CVSR (I_{dc} =200 mA)

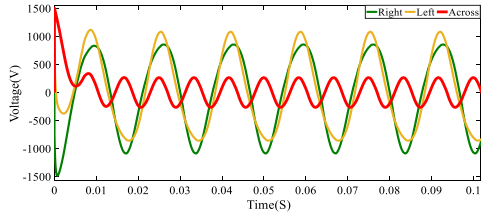

Fig18. Induced voltage across dc windings (I_{dc} =200 mA)

Increasing the dc bias to 2 A, causes enough dc offset for fluxes through the outer legs to drive the corresponding core legs into saturation (Figure 19). Therefore, the outer leg flux densities are no longer equal neither in terms of shape nor phase. At all times, the permeance of one of the outer legs is different than the other one. Therefore, the rate of change of the fluxes passing through the outer legs will be different and the induced voltage across the outer windings will not be zero. Since the inductions through the outer legs are distorted, the inductions through the middle leg would not be pure sine and we have a distortion in induced voltage across ac winding too, same as in the previous scenario.

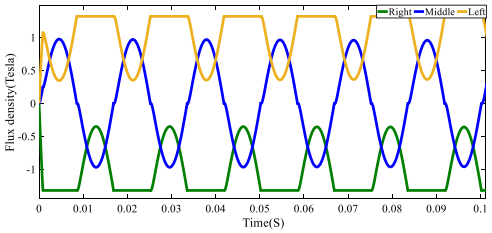

Fig19. Flux densities through CVSR (I_{dc} =2A)

In Figure 20, the induced voltage across the ac winding is shown at a dc bias of 10A. Since the bias is very high, the core is deeply saturated. The ac flux density through the center leg is small due to the high reluctance of the outer legs. So, the induced voltage across the ac winding is also small. The flux density through all the legs, the induced voltage across dc winding, and the current through the ac winding are all similar to the scenario at 10A dc bias without hysteresis.

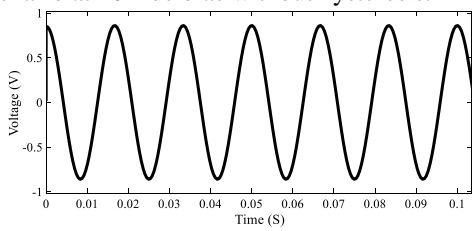

Fig20.Induced voltage across ac winding (I_{dc} =10A)

V. CONCLUSIONS

This paper presents an improved Gyrator-Capacitor (G-C) model by considering hysteresis, in addition to core saturation, in order to provide better accuracy in the modeling of power magnetic devices. The G-C approach provides a different analogy between the magnetic and the electric circuits. With this approach, capacitors that are equivalent to magnetic permeances can be nonlinear to model the core saturation. In addition, a resistor added in series to the capacitor can model the core hysteresis. Results from simulations of an improved G-C model of a three-legged Continuously Variable Series Reactor (CVSR), under nominal conditions and for different values of dc bias current are presented, with a comprehensive analysis of the CVSR behavior. Future work will investigate a more complicated and realistic model of the device and its behavior during transient conditions.

REFERENCES

[1] S. R. Khazeiynasab and J. Qi, "Generator Parameter Calibration by Adaptive Approximate Bayesian Computation with Sequential Monte Carlo Sampler," in *IEEE Transactions on Smart Grid*, *2021*.

[2] D. C. Hamill, "Gyrator-capacitor modeling: a better way of understanding magnetic components," *Proceedings of 1994 IEEE Applied Power Electronics Conference and Exposition - ASPEC'94*, Orlando, FL, USA, 1994, vol.1, pp. 326-332.

[3] M. Hayerikhiyavi and A. Dimitrovski, "Gyrator-Capacitor Modeling of A Continuously Variable Series Reactor in Different Operating Modes," *2021 IEEE Kansas Power and Energy Conference (KPEC)*, 2021.

[4] M. Hayerikhiyavi and A. Dimitrovski. "Comprehensive Analysis of Continuously Variable Series Reactor Using GC Framework". arXiv preprint arXiv:2103.11136. 2021 Mar 20.

[5] Valadkhan S, Morris K, Khajepour A. "Review and Comparison of Hysteresis Models for Magnetostrictive Materials". *Journal of Intelligent Material Systems and Structures. 2009*;20(2):131-142.

[6] M. F. Jaafar and M. A. Jabri, "Study and modeling of ferromagnetic hysteresis," *2013 International Conference on Electrical Engineering and Software Applications, 2013*, pp. 1-6

[7] A. Dimitrovski, Z. Li, and B. Ozpineci, "Applications of saturable-core reactors (SCR) in power systems," presented at the IEEE Power Energy Soc. T&D Conf. Expo., Chicago, IL, USA, 2014.

[8] A. Dimitrovski, Z. Li, and B. Ozpineci, "Magnetic amplifier-based power flow controller," IEEE Trans. Power Del., vol. 30, no. 4, pp. 1708–1714, Aug. 2015.

[9] M. Young, A. Dimitrovski, Z. Li and Y. Liu, "Gyrator-Capacitor Approach to Modeling a Continuously Variable Series Reactor," *IEEE Trans. on Power Delivery*, vol. 31, no. 3, pp. 1223-1232, June 2016.

[10] M. Young, Z. Li and A. Dimitrovski, "Modeling and simulation of continuously variable series reactor for power system transient analysis," *2016 IEEE Power and Energy Society General Meeting (PESGM), Boston*, MA, 2016, pp. 1-5.

[11] E. Rozanov, S. Ben-Yaakov," Analysis of Current-controlled Inductors by New SPICE Behavioral Model," *HAIT Journal of Science and Engineering*, vol. 2, pp. 558-570.

[12] S. D. Sudhoff, "Magnetics and Magnetic Equivalent Circuits," in Power Magnetic Devices: A Multi-Objective Design Approach. Wiley-IEEE Press, 2014, pp. 45–112.

[13] "MATLAB - MathWorks - MATLAB & Simulink." [Online]. Available: https://www.mathworks.com/products/matlab.html

[14] G. M. Shane and S. D. Sudhoff, "Refinements in anhysteretic characterization and permeability modeling," *IEEE Transactions on Magnetics*, vol. 46, no. 11, pp. 3834–3843, 20.01